Towards correlative super-resolution fluorescence and electron cryo-microscopy

Georg Wolff[1], Christoph Hagen[1], Kay Grünewald[1], Rainer Kaufmann[1,2,*]

[1]Division of Structural Biology, Wellcome Trust Centre for Human Genetics, University of Oxford, Oxford, United Kingdom

[2]Department of Biochemistry, University of Oxford, Oxford, United Kingdom

[*]To whom correspondence should be addressed: rainer@strubi.ox.ac.uk

Running Title: Towards super-resolution cryo-CLEM

Key Words: cryo-CLEM, cryo-imaging, nanoscopy, SRM, TEM

Abstract

Correlative light and electron microscopy (CLEM) has become a powerful tool in life sciences. Particularly cryo-CLEM, the combination of fluorescence cryo-microscopy (cryo-FM) permitting for non-invasive specific multi-colour labelling, with electron cryo-microscopy (cryo-EM) providing the undisturbed structural context at a resolution down to the Ångstrom range, has enabled a broad range of new biological applications. Imaging rare structures or events in crowded environments, such as inside a cell, requires specific fluorescence based information for guiding cryo-EM data acquisition and/or verify the identity of the structure of interest. Furthermore, cryo-CLEM can provide information about the arrangement of specific proteins in the wider structural context of their native nano-environment. However, a major obstacle of cryo-CLEM currently hindering many biological applications is the large resolution gap between cryo-FM (typically in the range of ~400 nm) and cryo-EM (single nanometre to Ångstrom range). Very recently, first proof of concept experiments demonstrated the feasibility of super-resolution cryo-FM imaging and the correlation with cryo-EM. This opened the door towards super-resolution cryo-CLEM, and thus towards direct correlation of structural details from both imaging modalities.

Introduction

Fast freezing techniques (vitrification) provide immobilization of biological samples embedded in amorphous ice, thus preserving the structures in their native state (Dubochet et al., 1988). This sample preparation method with its advantages over chemical fixation has been used in structural (cell) biology for already a few decades (Dubochet, 2012). Recently undergoing a "resolution revolution" (Kühlbrandt, 2014), electron cryo-microscopy (cryo-EM) can resolve biological structures down to the atomic level (Rodriguez et al., 2015; Glaeser, 2016). Identifying and locating particles or structures of interest within a crowded sample at such high resolutions and without specific labelling presents a major challenge. This has led to the implementation of correlative light and electron cryo-microscopy (cryo-CLEM), particularly the combination of cryo-EM with fluorescence cryo-microscopy (cryo-FM) which allows labelling and identifying specific proteins or structures in vitreous samples (Sartori et al., 2007; Schwartz et al., 2007). Technical improvements of the cryo-stages used for cryo-FM imaging over the last decade enabled rather routine cryo-CLEM measurements (Briegel et al., 2010). However, the optical resolution in the fluorescence images is limited to a range of 400-500 nm mainly due to the lack of immersion cryo-objectives (Schellenberger et al., 2014).

In 2014 Eric Betzig, Stefan W. Hell and William E. Moerner were awarded the Nobel Prize in Chemistry for their pioneering work of super-resolution fluorescence microscopy - marking another ongoing contemporary revolution (Weisenburger and Sandoghdar, 2015). However, whether the concepts of super-resolution could be applied to overcome the very limited resolution of cryo-FM was long unknown due to altered fluorophore characteristics at low temperatures (for review see Kaufmann et al. (2014a)). Very recently, first proof of concept experiments were reported demonstrating the feasibility of super-resolution cryo-FM and also possible ways towards the correlation with cryo-EM (Chang et al., 2014; Kaufmann et al., 2014b; Liu et al., 2015). It has been demonstrated that super-resolution cryo-FM can be utilized to identify structures below the diffraction limit and thus, for instance, discern different developmental/conformational states of macromolecular complexes in the crowded interior of a bacterial cell, which was not achievable with conventional cryo-CLEM (Chang et al., 2014). However, many routes to access resolution beyond the diffraction limit of light in cryo-FM remain unexplored, and a variety of technical challenges have to be overcome to exploit the full potential of this new methodology. In this review we highlight the challenges

and prospects of super-resolution cryo-CLEM in the context of the current state of the art regarding technical and photo-physical considerations.

Sample preparation for cryo-microscopy – a primer

Sample preparation and handling in cryo-FM relies on methods and sophisticated instrumentation originating mainly from cryo-EM. The latter imaging technique is becoming a major player in structural biology (Callaway, 2015; Subramaniam et al., 2016), recently distinguished as "Method of the Year 2015" (Eisenstein, 2016). Particularly the field of single particle cryo-EM, a technique where thousands of individual but identical particles are imaged, aligned and averaged, is benefiting greatly from the introduction of direct electron detectors into electron microscopes (Egelman, 2016). Near-atomic resolution can be reached, which was previously only possible by X-ray crystallography or NMR-spectroscopy (Nogales, 2016). Another popular modality of cryo-EM is electron cryo-tomography, the method of choice for obtaining 3D images with a resolution in the single-nm range for cellular structures, and at even higher resolution for isolated macromolecular assemblies by sub-tomogram averaging (Bharat et al., 2015; Schur et al., 2015; Irobalieva et al., 2016).

To analyse unperturbed biological structures with cryo-EM, cryo-immobilization is needed to preserve a near-native state of the sample, especially by keeping the water in its structural context. For cryo-immobilization it is crucial to freeze the aqueous biological sample very fast in order to avoid crystallization of the water molecules and to yield an amorphous, vitreous state (Dubochet, 2007). Liquid nitrogen (LN_2) is not suitable as a cryogen, since it does not allow rapid heat transfer (Dobro et al., 2010) and thus causes crystallization (Taylor and Glaeser, 1974; Dubochet, 2016). First successful vitrification of water droplets was achieved by using liquid n-heptane or liquid ethane as cryogen (Brüggeller and Mayer, 1980; Dubochet and McDowall, 1981).

Today there is a variety of cryo-preparation methods to choose from, depending on how a sample should be vitrified and for what purpose (Mielanczyk et al., 2014). Plunge freezing of thin-blotted samples on carbon-coated EM grids with a gravity driven plunger into LN_2-cooled ethane or a mixture of propane and ethane is widely used (Tivol et al., 2008), even under field conditions (Comolli et al., 2012). Commercial instruments enabling automation and environmental control of the blotting process help to prepare specimens reproducibly for research in the field of structural (cell) biology using cryo-EM. Examples are: the Vitrobot™ (FEI, Hillsboro, OR, USA), introduced in 2005 (Frederik and Hubert, 2005); the Gatan CP3 (Gatan, Pleasanton, CA, USA); or the Leica EM GP (Leica, Vienna,

Austria), the latter blotting from one side of the specimen holder and thus being especially suitable for cellular samples (Resch et al., 2011). Automated inkjet-like dispense systems (Jain et al., 2012), time-resolved mixing of reagents (Lu et al., 2009) or the array-type application of multiple samples on a single EM grid (Castro-Hartmann et al., 2013) only mark the beginning of developments towards even more sophisticated sample preparation and automation protocols in cryo-EM (Glaeser et al., 2016; Tan et al., 2016).

Beside plunge freezing, which can vitrify only thin samples (up to 5-15 µm thickness, see also Mejia et al. (2014)), high pressure freezing allows vitrification of thicker specimen like bulk cells or tissue samples (Riehle and Hoechli, 1973; Moor, 1987). This is achieved through super-cooling by applying pressure of about 2100 bar for a few milliseconds before flash-freezing. The applied high pressure avoids ice crystal formation by lowering the freezing point of water, enabling vitrification for sample thicknesses of up to 200 µm (McDonald, 2014). Unfortunately, for transmission electron microscopy ice layers thicker than 1 µm are not readily accessible, thus typically limiting tomographic approaches in practise to ~500-800 nm maximum samples thickness (Lučić et al., 2005). Electron cryo-microscopy of vitreous sections (CEMOVIS) addresses this issue, by slicing 10-200 nm thin sections of an aqueous frozen sample (Al-Amoudi et al., 2004; Han et al., 2008), which then can be observed by cryo-EM revealing intracellular structures like proteins inside organelles, or in the nucleus. Recently, another technique for generating sections of vitreous biological specimens was introduced: focused ion beam (FIB) milling (Marko et al., 2006). For FIB milling typically gallium ions are used for the abrasion of thicker specimen to subsequently observe them in a transmission electron microscope (Rigort and Plitzko, 2015). Compared to other cryo-sectioning methods, guidance from the scanning electron microscopy imaging allows localizing larger targets and then to mill very precisely uniform lamellae of 150-500 nm thickness. However, targeting rare events or small structures within a cell remains challenging and requires advanced correlative approaches (Arnold et al., 2016).

Fluorescence cryo-microscopy and cryo-CLEM – state of the art and limitations

The correlation of cryo-FM with cryo-EM is a growing technique that allows targeting (rare) objects or events using specific fluorescence labelling (de Boer et al., 2015; Fonta and Humbel, 2015; Timmermans and Otto, 2015).

Dedicated cryo-stages allow fluorescence imaging of vitreous samples on standard fluorescent microscopes (Briegel et al., 2010; Carlson and Evans, 2011; Jun et al., 2011). One of the first cryo-stages to observe frozen-hydrated samples with fluorescence microscopy was

developed in 2007 for an inverted microscope setup (Sartori et al., 2007). An improved and commercialized second generation termed Cryostage² was developed in cooperation with FEI (Eindhoven, The Netherlands) and released three years later (Rigort et al., 2010). With this stage, working distances of objective lenses below 2 mm are possible, an automated LN_2 pump system keeps the samples below the devitrification temperature and a slider holding up to four frozen-hydrated EM grids, which can also handle Autogrid cartridges (FEI), is stabilizing the handling and transfer of the rather fragile EM grids (Rigort et al., 2010). In parallel, a cryo-stage for upright microscopy had been developed, cooling the sample not with LN_2, but with cold N_2 gas to achieve reduced vibrations (Schwartz et al., 2007). This stage later was commercialized by Instec (Boulder, CO, USA), known as model CLM77K, also available as a version for inverted microscopes (model CLM77Ki). However, for the upright microscope version working distances of the used objective lens are in the range of 5 mm to prevent devitrification of the sample. An already existing heating and freezing microscope stage by Linkam Scientific Instruments (Surrey, UK) modified for the observation of vitreous samples (van Driel et al., 2009) was the initial step in the development of a commercial cryo-stage, yielding the second generation Linkam cryo-stage CMS196. This stage fits most upright light microscopes, supports multiple types of specimen holders and contains an integrated LN_2 Dewar, so no mechanical connection to pumping systems is necessary for short-term image acquisitions (Carzaniga et al., 2014). Additional cooling of the objective allows for shorter working distances, and thus higher numerical aperture (NA), as has been demonstrated for a 0.9 NA objective lens with 300 µm working distance and dry ice cooling (Schorb and Briggs, 2014). Recently Leica Microsystems (Vienna, Austria) introduced a cryo-stage for upright microscopes based on the prototype by Schorb and Briggs (2014), which has a decoupled LN_2 reservoir to reduce vibrations originating from boiling nitrogen or pumping processes. The included cryo transfer system allows sample transfers with low ice contamination. The design of an air objective lens improved for cryo-FM allows an NA of 0.9 with a relatively short working distance of 280 µm, which is achieved by less heat conducting materials in the front part of the objective body (Strnad et al., 2015). Most recently, the CorrSight system (FEI, Gräfelfing, Germany), a cryo-stage for an inverted microscope setup, has been described (Arnold et al., 2016). This system also enables using a 0.9 NA objective lens with the advantage that the objective is separated by a glass window from the cold environment, which allows to use any air objective with a working distance of >410 µm and correction for a standard glass coverslip.

However, a major problem for advanced cryo-imaging of current, both commercial and the various experimental cryo-stages, is mechanical/thermal instability. Alternative design concepts have addressed this issue by combining the thermal and mechanical stability of a cryostat with a sample exchange mechanism to enable insertion of vitreous samples, but creating additional limitations regarding the performance of objective lenses, and thus impairing resolution and sensitivity (Hussels et al., 2012; Li et al., 2015b). Hussels et al. (2012) used air objective lenses which had been designed for ambient temperature, but were still suitable for imaging at 1.6 K. A relatively simple optical design allows a very broad operation range, but typically is associated with chromatic and/or spherical aberrations if a high NA is desired. Li et al. (2015b), on the contrary, placed the objective outside of the cryostat at ambient temperature, which allows making use of more complex and highly corrected air objectives. However, due to the relatively thick quartz glass window in the cryostat, a long working distance air objective was required that could correct for the aberrations caused by the window, and which restricted the achievable NA to 0.7 (Li et al., 2015b).

A major limitation, especially for super-resolution cryo-FM, is the low NA of suitable air objective lenses in current cryo-stages, as described above. The most important factor for achieving maximum resolution with super-resolution methods in general is the signal to noise ratio, which is mainly determined by the number of detected photons per fluorescent molecule, to distinguish signal from background noise. Photon detection efficiency of an optical setup is quadratically proportional to the NA of the objective. Therefore, in cryo-FM the lack of immersion objectives not only results in reduced resolution for wide-field or confocal applications, but also severely limits the detection efficiency (30-60% compared to 1.3 NA), and thus the achievable resolution for super-resolution cryo-approaches. Using a reflecting objective, recently a cryo-FM approach achieved an NA of 0.99 (Inagawa et al., 2015). However, to realize localization precisions close to or below one nanometre, more than 10^6 photons have to be collected per fluorophore, still resulting in acquisition times exceeding one hour with an NA <1.0 (Weisenburger et al., 2014; Inagawa et al., 2015; Li et al., 2015b). First proof of concept experiments demonstrated the technical feasibility of a cryo-microscope with immersion objectives (Le Gros et al., 2009). The rather simple optical design of the objective lens used in this study prevented total mechanical failure (breakage of relevant parts during cooling/warming). However, the point spread function (PSF) measurements published for this system indicate that so far the resolution did not exceed the

resolution of other systems with air objectives mounted outside the cryo-stage at ambient temperatures (Smith et al., 2014).

Even if reaching an NA >1.0 in cryo-FM, this will be associated with further challenges for high demanding applications like super-resolution imaging. Under cryo-conditions, structures, but also fluorophores in the sample, are in a spatially fixed state causing the emitted light to be in a distinct polarization, which can result in an asymmetric PSF (Gould et al., 2008; Weisenburger et al., 2014). To avoid this effect leading to single molecule localization errors of ~100 nm when the fluorophore is 200 nm out of the focal plane, an azimuthal polarization filter can be integrated into the detection path of the microscope (Lew and Moerner, 2014). However, the use of this filter reduces the photon yield by 30-75%, depending on the fluorophores orientation (Lew and Moerner, 2014). On the contrary, if not corrected for, this feature could possibly even be exploited in the further development of super-resolution cryo-FM to gain information about the orientation of molecules, for example in single particle studies to identify conformational changes.

Currently, the state of the art in cryo-CLEM for locating a fluorescent signal and correlating it with the cryo-EM image is an overall correlation precision in the range of 50-100 nm, which has been demonstrated in proof of principle experiments (Schellenberger et al., 2014; Schorb and Briggs, 2014). However, to identify specific structures in crowded environments, where for example many similar objects are close together, it is inevitable to reach even higher localization and correlation accuracies. In cases where the labelled structures are densely packed, i.e. distances below the resolution of the cryo-FM imaging system, super-resolution cryo-FM is required to distinguish structures on the nanometre scale (Chang et al., 2014). For cryo-CLEM in the field of single particle cryo-EM even sub-nanometre precision might be necessary, for example to determine different protein domains and their conformation or orientation.

Super-resolution fluorescence microscopy – the basics

Super-resolution fluorescence microscopy comprises techniques to overcome the diffraction limit of light, which is ~200 nm for the visible spectrum (for recent reviews, see Fornasiero and Opazo (2015), Hell et al. (2015) and Sydor et al. (2015)). The first concepts and optical setups for super-resolution fluorescence imaging have been developed already in the 1990s, such as the 4Pi (Hell and Stelzer, 1992; Hell et al., 1994), the I^5M microscope (Gustafsson et al., 1995) and stimulated-emission-depletion (STED) microscopy (Hell and Wichmann, 1994). The latter, which is currently one of the major super-resolution methods for biological

applications, is based on a point scanning confocal setup. In every scanning step the diffraction-limited volume of excited fluorophores is depleted by a doughnut-shaped red-shifted STED beam to inactivate off-centre fluorophores. The volume of the remaining fluorescent molecules is dependent on the intensity of the STED beam, and thus allows fluorescence detection of features significantly smaller than the diffraction limited excitation volume (Hell and Wichmann, 1994). By scanning the whole region of interest a super-resolution image of the sample is generated. 3D super-resolution imaging with STED microscopy can be achieved by 3D shaping of the depletion PSF (Wildanger et al., 2009). By tuning the resolution via the intensity of the depletion laser and varying the scanned area or volume, the balance between spatial and temporal resolution can be adjusted for the individual requirements (Hell, 2009). For small fields of views (~2 x 2 µm²) in 2D STED live-cell imaging, 28 frames per second have been achieved for a resolution of 62 nm (Westphal et al., 2008), whereas larger areas (20 x 20 µm) and higher spatial resolution (40 nm) require longer acquisition times (10 s) for one STED image (Hein et al., 2010).

A very different technique, structured illumination microscopy (SIM), that allows resolution beyond the diffraction limit was introduced around the same time as STED microscopy (Heintzmann and Cremer, 1999; Gustafsson, 2000). SIM utilizes a striped illumination pattern to improve the resolution up to a factor of two in comparison to conventional fluorescence microscopy. The interaction of the excitation pattern with the sample enables to detect higher spatial frequency information that is shifted to lower frequencies accessible to the optical imaging system. However, as the excitation pattern is still limited by diffraction, the resolution improvement is hence limited to 2x and a higher resolution is only possible by using saturation (non-linear) effects of switchable fluorophores (Gustafsson, 2005). The advantage of standard (linear) SIM compared to other super-resolution techniques is that no switching or depletion of the fluorophores is necessary, and thus relatively low laser intensities can be used, which is highly beneficial for the sample with regards to phototoxicity, particularly in live-cell imaging. With already demonstrated 16 frames per seconds it is a rather fast super-resolution imaging technique (Xu et al., 2013).

Single molecule localization microscopy (SMLM) is currently perhaps the most used super-resolution technique for biological applications. It has been developed a few years after SIM and STED and was first introduced as stochastic optical reconstruction microscopy (STORM) (Rust et al., 2006), (fluorescence) photoactivated localization microscopy ((F)PALM) (Betzig et al., 2006; Hess et al., 2006). In general, SMLM is based on the principle of localizing single fluorescent molecules by utilizing their capability of being

switched between a bright and a dark state (or spectrally different states) to separate their signals over time, and thus in space. The positions of these isolated single molecule signals can be determined with a precision much higher than the optical resolution of the imaging system, which enables the reconstruction of a super-resolution image of the underlying fluorophore distribution. (F)PALM typically uses photo-activatable fluorophores, which results in a single and irreversible on and off switching event of the molecule (Betzig et al., 2006; Hess et al., 2006). STORM is based on reversibly switchable fluorophores, which can be switched multiple times between the ON and the OFF state (Rust et al., 2006). Later developments demonstrated SMLM using light induced photo-switching capabilities of conventional fluorescent proteins and organic dyes: direct STORM (dSTORM) (Heilemann et al., 2008), spectral position determination microscopy (SPDM) (Lemmer et al., 2008) and ground state depletion followed by individual molecule return (GSDIM) (Fölling et al., 2008). The different methodological modalities and wide range of suitable fluorophores make SMLM a very versatile and broadly used super-resolution technique, which can achieve resolutions down to the 10 nm range (Aquino et al., 2011; Xu et al., 2012).

All super-resolution methods face the challenge of live-cell imaging. Typically, a compromise between spatial and temporal resolution is required due to relatively long data acquisition times (Westphal et al., 2008; Jones et al., 2011; Shao et al., 2011; Huang et al., 2013; Li et al., 2015a). The acquisition rate is not only limited by the specifications of the detector, but also by the photo-physics/chemistry of the fluorophores (e.g. photo-switching speed, photon budget and relaxation times), and thus the vast majority of current super-resolution FM is performed in chemically fixed cells (Betzig, 2015). Chemical fixation is used to immobilize the structures of interest for achieving maximum spatial resolution. However, this can cause structural artefacts in the sample (Morgenstern, 1991; Bleck et al., 2010), particularly at the level of resolution accessible and interpreted by using super-resolution methods (Weinhausen et al., 2014; Betzig, 2015). It also has been shown, that chemically fixed tissues lost about a third of their volume compared to cryo-fixed samples (Korogod et al., 2015). This highlights that structural preservation is as important as resolution. A superior alternative to chemical fixation is cryo-immobilizing of the sample by vitrification.

Super-resolution microscopy under cryo-conditions and its compatibility with vitreous samples and cryo-EM

Super-resolution imaging under cryo-conditions is a very new field of microscopy and most of the boundary conditions are currently unknown (Kaufmann et al., 2014a). Altered fluorophore characteristics at low temperatures (Creemers et al., 2000; Moerner, 2002; Zondervan et al., 2003; Faro et al., 2010) are a big challenge for super-resolution cryo-FM, but could also offer certain advantages over imaging at ambient temperatures. On the one hand, photo-bleaching and photo-decomposition of fluorophores is substantially reduced or could even be eliminated under cryo-conditions (Moerner and Orrit, 1999; Sartori et al., 2007; Schwartz et al., 2007; Le Gros et al., 2009; Li et al., 2015b). On the other hand, photo-switching, a crucial characteristic for most super-resolution techniques, can still be observed for many fluorophores at low temperatures, but might be drastically changed compared to ambient temperatures (Creemers et al., 2000; Moerner, 2002; Zondervan et al., 2003; Faro et al., 2010; Weisenburger et al., 2013; Chang et al., 2014; Kaufmann et al., 2014b; Liu et al., 2015). Furthermore, the relatively high laser intensities used in super-resolution methods for photo-switching or fluorescence depletion can cause local devitrification of the sample resulting in the formation of crystalline ice, potentially destroying the biological sample (Chang et al., 2014; Liu et al., 2015; Huebinger et al., 2016). For an overview of challenges and prospects of super-resolution cryo-FM see Fig. 1.

Cryo-SIM

SIM could directly benefit from the substantially reduced photo-bleaching under cryo-conditions to overcome one of the major drawbacks of SIM. Cryo-SIM would be unaffected by the changed photo-switching characteristics of fluorophores, and thus would mainly benefit from imaging under cryo-conditions regarding the fluorophore behaviour. Furthermore, the excitation intensities do not necessarily need to be very high such as for photo-switching fluorescent molecules in SMLM or the fluorescence depletion in STED microscopy. This would be highly beneficial for keeping the sample in a vitreous state. However, optical limitations of current cryo-microscopes would still apply, as to all other super-resolution imaging modalities. As SIM is fundamentally limited to a maximum resolution improvement of 2x in all directions, cryo-SIM would currently (i.e. without a dedicated immersion cryo-objective) be able to achieve a lateral resolution of only ~180 nm (~650 nm axially) and could from this aspect alone not add significant value in comparison to fluorescence imaging at ambient temperatures. However, cryo-SIM would find many applications in the cryo-CLEM field, particularly for 3D correlation/targeting for cryo-FIB milling of lamellae in cellular samples (Arnold et al., 2016). For achieving optimal

performance in cryo-EM/tomography, a lamella thickness of ~300 nm or even less is pursued (Rubino et al., 2014). Very recently, it has been demonstrated that correlation accuracies of 200-300 nm are possible using 3D cryo-FM imaging and fiducial markers which give high signals in fluorescence and back-scattered electrons images (Arnold et al., 2016). However, if structural information is required in cryo-FM (e.g. to identify/distinguish specific structures) super-resolution cryo-FM techniques are required (Arnold et al., 2016). Particularly the improvement of resolution and contrast in the z-direction of cryo-SIM and cryo-Airyscan could be of advantage for applications in thick vitreous samples requiring FIB milling (Fig. 2). Similarly, 3D correlation in the thicker samples of soft X-ray cryo-microscopy might be another potential field of application (Schneider et al., 2012; Do et al., 2015).

Cryo-Airyscan

The Airyscan principle for confocal microscopes is a method which allows to enhance the resolution of up to a factor of 1.7 compared to conventional confocal imaging, similar to SIM, in all 3 dimensions (Tychinskii et al., 1997; Engelmann et al., 2014). It uses information usually cut off by the pinhole in regular confocal microscopes to reconstruct the image (Tychinskii et al., 1997; Engelmann et al., 2014). Higher photon-doses, necessary for confocal scanning microscopy, lead to faster bleaching and longer image acquisition times compared to SIM. However, not only the simpler instrument design, but also the fact that the Airyscan system has already been tested under cryo-conditions for correlative FIB approaches using the Linkam cryo-stage (Rigort et al., 2015b), makes it highly competitive to cryo-SIM. In a first cryo-Airyscan approach a resolution improvement of 1.4 and a substantially increased contrast compared to confocal cryo-imaging, has been demonstrated (Rigort et al., 2015a).

Cryo-STED

STED under cryo-condition has been demonstrated in a first proof of concept experiment achieving an increase in resolution by the factor of 1.6 (Giske, 2007) compared to the same optical conditions at ambient temperatures. Low temperatures allow for using wavelengths with higher STED efficiencies, as anti-Stokes excitation is absent in cryo-conditions (Giske, 2007). However, in the approach of Giske (2007), the samples were slowly cooled down by the cryostat and therefore did not reach a vitreous state. Also considerable for cryo-approaches is that the depletion beam intensities necessary for STED are typically in a range of MW/cm²-GW/cm², which might be a problem for keeping the vitreous sample below the

devitrification point. It has been shown that laser intensities of 300 W/cm² (wide-field illumination) for 1-2 minutes can warm up an amorphous ice sample and cause crystal formation and thus change or even destroy biological structures (Chang et al., 2014). Whether the photon-dose of the picoseconds-short but very intense scanned STED beam keeps the sample below the devitrification point, and thus would allow cryo-STED imaging of vitreous samples and correlation with cryo-EM, remains to be investigated.

Cryo-ESS

Very recently a new method, ESS (exited state saturation) microscopy, has been reported that uses the saturation effect of fluorescent molecules, somewhat similar to the principle of STED, for resolving individual single molecules at low temperatures with much higher resolution than the diffraction limit (Yang et al., 2015). However, for multiple molecules located within the excitation spot (diameter ~1 µm) the contrast is decreased (Yang et al., 2015), thus currently leaving open the question whether this method would be conceptually suitable for super-resolution cryo-FM.

Cryo-SMLM

So far, SMLM under cryo-conditions is the only super-resolution fluorescence microscopy technique which has been applied to vitreous samples (Chang et al., 2014; Kaufmann et al., 2014b; Liu et al., 2015). Using long working distance air objective lenses with NAs of 0.75-0.8, resolutions in a range of 75-125 nm have been achieved with cryo-SMLM in cellular samples (Kaufmann et al., 2014b; Liu et al., 2015). The combination of cryo-SMLM with cryo-EM has been demonstrated, but so far with substantial sacrifices for one or the other imaging modality (Chang et al., 2014; Liu et al., 2015). Achieving maximum resolution for cryo-SMLM is typically linked to devitrification of the sample that is caused by the relatively high laser intensities used for the photo-switching of the fluorescent molecules (Chang et al., 2014; Liu et al., 2015), and thus currently hindering a wider application of this super-resolution approach in correlation with cryo-EM. Chang et al. (2014) achieved suitable EM imaging quality, whereas poor photo-switching of the fluorescent protein PA-GFP (Patterson and Lippincott-Schwartz, 2002) under cryo-conditions allowed only for a moderate resolution improvement on the cryo-FM side (<2x). Besides non-continuous laser exposure to allow for heat dissipation, the use of cryo-protectants (10% Ficoll PM 70 and 10% ethylene glycol) in the sample helped to increase the devitrification temperature threshold, but laser intensities for photo-switching still had to be kept relatively low (300

W/cm^2) to prevent devitrification of the sample (Chang et al., 2014). Cryo-protectants might be a suitable method for osmotically robust cells like bacteria (Chang et al., 2014), but not for mammalian cells. Furthermore, cryo-protectants in general decrease the contrast in cryo-EM. Very low contrast cryo-EM images were precisely the issue in the alternative approach of super-resolution cryo-CLEM by Liu et al. (2015), who demonstrated a resolution of 75 nm in cryo-SMLM with the fluorescent protein Dronpa (Ando et al., 2004). Formvar-coated EM grids, which absorb less light (heat), had been explored as an alternative to the typically used carbon-coated grids to allow for higher laser intensities (1.75 kW/cm^2), and thus for improved photo-switching and consequently a higher resolution in cryo-SMLM (Liu et al., 2015). However, this substantially lowered the compatibility with cryo-EM due to the high electron absorption of the formvar film and accordingly reduced contrast and resolution.

To overcome mechanical instabilities of the setup in cryo-SMLM imaging, drift correction during or after cryo-SMLM data acquisition using fiducial markers or bright fluorescent background structures has been demonstrated, but the remaining error was on the order of the average single molecule localization precision (Kaufmann et al., 2014b; Liu et al., 2015). An active feedback system for drift correction was used by Liu et al. (2015), which enabled a 5 nm precise correction in lateral directions.

SMLM offers, besides resolution improvement, single molecule information that can be used for further quantitative analysis of the data. This makes cryo-SMLM an ideal candidate for the investigation of protein arrangements and distributions in the structural context provided by cryo-EM (Fig. 2).

Ultra-high-precision localization cryo-microscopy

For certain applications of CLEM, structure-resolving super-resolution FM is not necessary and the precise location of a particle, a cellular compartment or a molecule is sufficient (e.g. in cases where rare objects or events are tagged with a fluorescent marker and no structural information is required in the fluorescence image). For isolated fluorescently labelled objects it is even possible to achieve a much higher localization precision than the resolution of super-resolution FM (compare Weisenburger et al. (2013); Weisenburger et al. (2014); Li et al. (2015b) and Kaufmann et al. (2014b), Liu et al. (2015)). For the latter, only the photons collected per one switching cycle of the molecule can be used for the position determination, whereas for optically isolated objects all photons are available which are emitted by the molecule(s) before irreversible photo-bleaching. Particularly under cryo-conditions, where irreversible bleaching is drastically reduced (Moerner and Orrit, 1999; Sartori et al., 2007;

Schwartz et al., 2007; Le Gros et al., 2009), it has been shown that single molecules can be localized with sub-nm precision (Weisenburger et al., 2013; Weisenburger et al., 2014; Li et al., 2015b), even the separation of two molecules with much smaller distance from each other than the FWHM of the PSF using their individual photo-blinking characteristics (Weisenburger et al., 2014). However, it remains to be demonstrated how well this method can be applied to vitrified biological samples which have typically a high background fluorescence compared to purified single molecules.

Localizing isolated fluorescent objects does not qualify as a (super-resolution) imaging technique, but could offer an important tool for the field of single particle cryo-EM, and therefore has been included for the sake of completeness. With localization precisions in the Ångstrom range, fluorescent information could here be used to support classification and averaging (Fig. 2).

Conclusions

Super-resolution cryo-FM is a promising technique opening up new perspectives, particularly for cryo-CLEM. It bridges the large resolution gap between two important imaging modalities which is currently hindering many biological applications. However, to unlock its full potential, a range of challenges have to be overcome.

Current cryo-stage designs lack high mechanical stability, which is a crucial requirement for super-resolution methods. Alternative design concepts have addressed this issue by combining the thermal and mechanical stability of a cryostat with a sample exchange mechanism, to allow for imaging vitreous specimens (Hussels et al., 2012; Li et al., 2015b). However, this impaired the performance of objective lenses, and hence the resolution and detection efficiency. Here, the development of an objective allowing immersion light microscopy under cryo-conditions could help to increase the photon yield in cryo-FM imaging drastically.

Besides technical obstacles, the very limited knowledge about the fluorophore characteristics at low temperatures on the single molecule level currently leaves both, advantages and disadvantages, for super-resolution cryo-FM in the dark. Here, cryo-SIM or cryo-Airyscan might offer solutions for super/enhanced-resolution cryo-CLEM, being mostly independent of changed photo-physics of the fluorophores and particularly suitable for applications where 3D information in a (fluorescently) crowded sample is required.

In a proof of concept demonstration it has been shown that cryo-STED could offer higher resolution than the ambient temperature equivalent (Giske, 2007). However, drift correction for scanning methods is not trivial and thus cryo-STED would require a very stable setup. Furthermore, STED typically uses very high laser intensities (Eggeling et al., 2013). For an application in the field of super-resolution cryo-CLEM, more investigations are required particularly regarding laser intensities and their effect on devitrification of the sample by a point scanning technique.

Although still in its infancy, cryo-SMLM is currently the only super-resolution method for which a correlation with cryo-EM has been achieved (Chang et al., 2014; Liu et al., 2015). The conceptual feasibility of super-resolution cryo-CLEM has been demonstrated, but so far the broad range of technical challenges and rather rudimentary knowledge about photo-switching under cryo-conditions is hindering a breakthrough of this approach. Besides the technical drawbacks of current setups impairing detection efficiency and mechanical stability, the problem of devitrification of the sample during cryo-SMLM data acquisition presents the biggest obstacle for routine correlation with cryo-EM. So far, correlative cryo-SMLM and cryo-EM has only been achieved by severe compromises on either the quality of cryo-SMLM (Chang et al., 2014) or cryo-EM imaging (Liu et al., 2015). Here, a general solution is required to address the problem of devitrification in a way that is suitable for all kind of samples typically imaged with cryo-EM, to enable a broad application of this technique.

Obviously, super-resolution cryo-CLEM with all its complexity is only justified as long as structural preservation is maintained. Super-resolution CLEM methods based on freeze substitution offer an alternative which presents a compromise between structural preservation, handling and imaging the samples at ambient temperatures that can be suitable and justified for answering certain biological questions not requiring preservation to the Ångstrom range (Watanabe et al., 2011; Johnson et al., 2015). Here, a battery of different staining and labelling techniques can be used known from classical EM of plastic sections, and the use of high NA immersion objectives and better mechanical stability increase the resolution of FM imaging. However, structural preservation is not as good as in vitreous samples, and other invasive procedures like heavy metal staining are required for contrasting (Bleck et al., 2010).

The full potential of imaging vitreous samples with super-resolution cryo-CLEM can only be unlocked by overcoming the current technical challenges. The various super-resolution methods are differently affected by changed fluorophore characteristics under

cryo-conditions (Fig. 1), but also offer different advantages and solutions to the broad range of potential applications in biology. Thus, cryo-SMLM would be an ideal method to correlate the distribution of a specific protein in its cellular context of the cryo-EM image, e.g. the distribution of ATPases in mitochondria (as indicated in Fig. 2; *cf.* Kühlbrandt (2015)). For the field of single particle analysis in cryo-EM, Ångstrom precision localization of fluorescently labelled particles might offer new possibilities for discriminating dynamic/conformational states of near-atomic resolved structures. Super-resolution cryo-FM, and thus also super-resolution cryo-CLEM, is clearly just at the beginning, but recent developments give a first glimpse of the enormous potential of this technique.

Figures

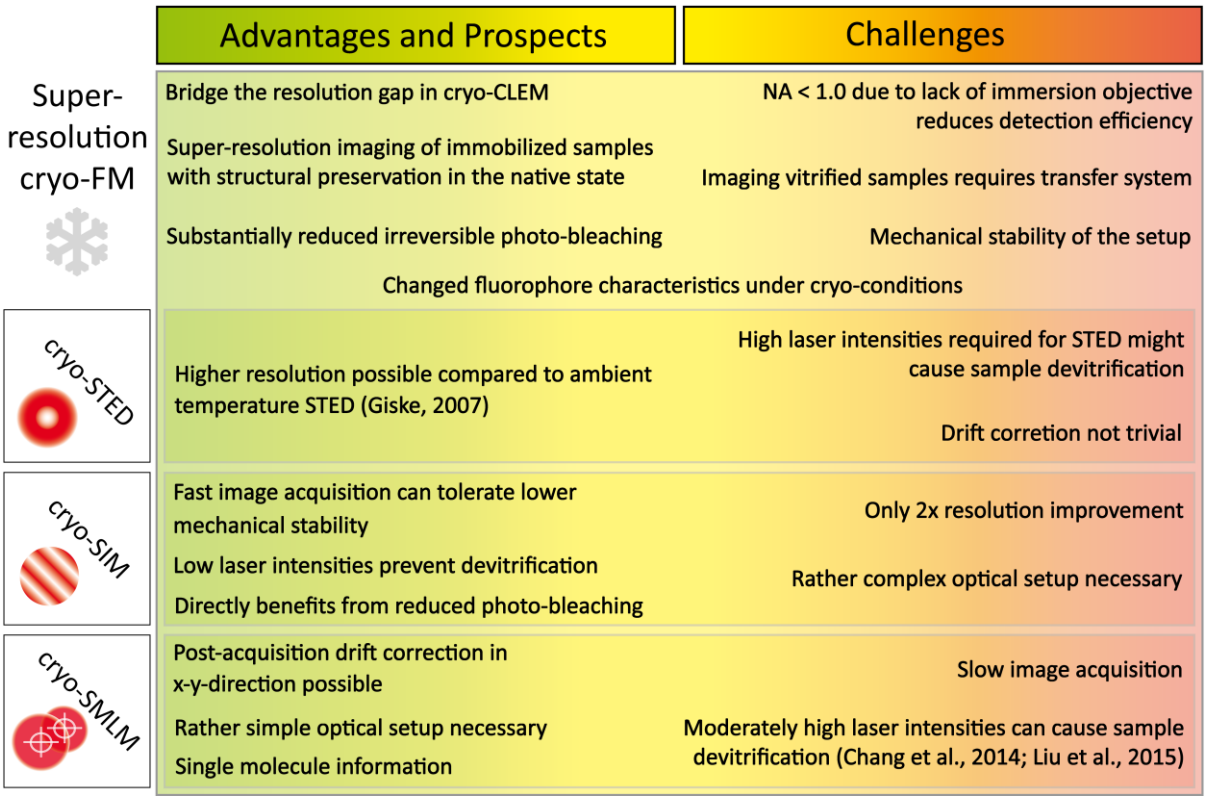

Figure 1. Comparison of key issues for super-resolution FM under cryo-conditions.

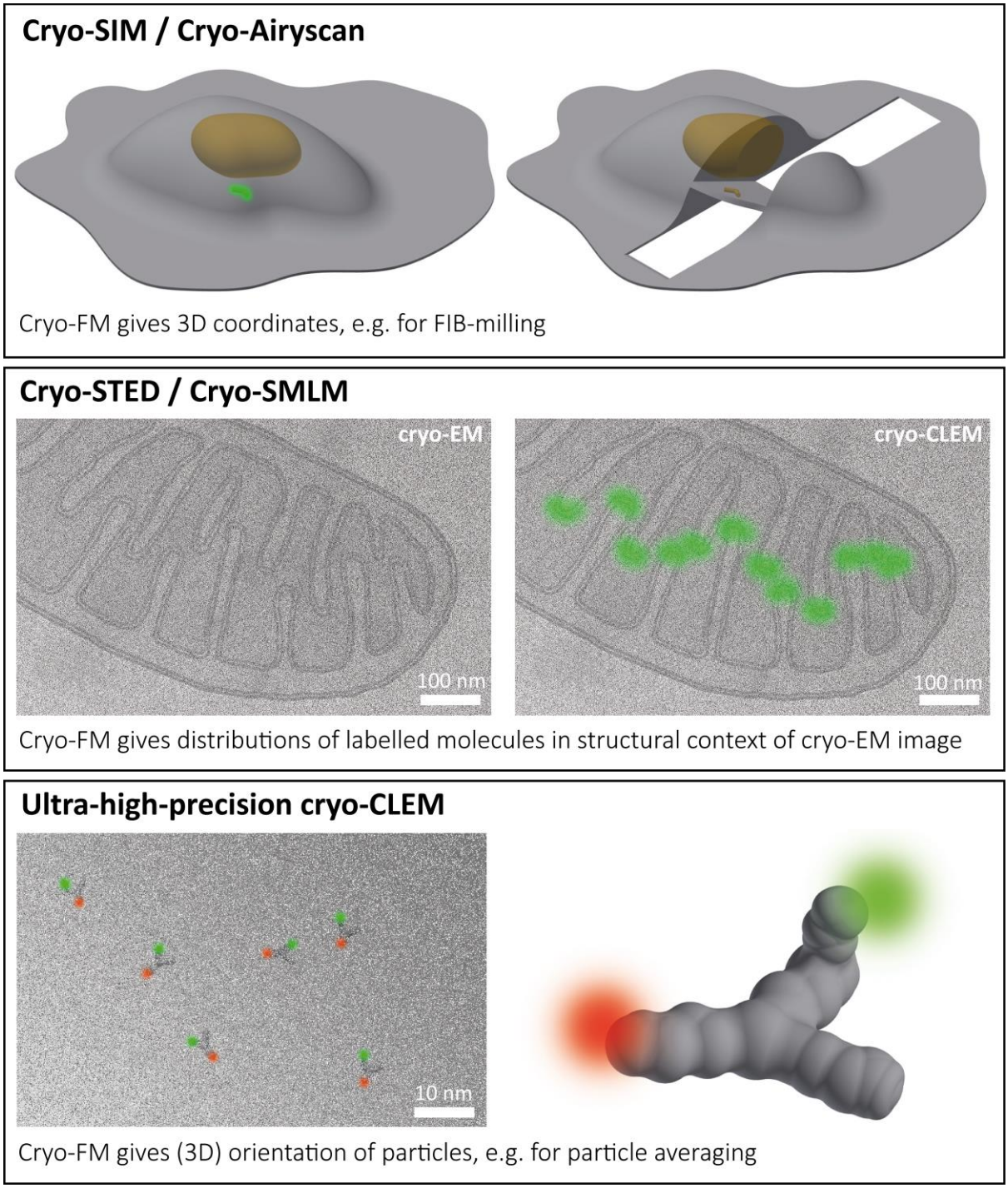

Figure 2. Illustrative application examples of different super-resolution cryo-FM approaches. Cryo-SIM and cryo-Airyscan provide advantages for 3D localization and correlation in thick samples for guiding FIB milling in case of rare objects/events, particularly in crowded environments such as cells. Cryo-STED and cryo-SMLM enable to achieve maximum resolution in cryo-FM, which can be applied for correlating protein distribution with the ultrastructural context of cryo-EM. Ultra-high-precision localization of single fluorescent markers on isolated particles will enable gaining information about the orientation and conformation of single particles from cryo-FM imaging to assist particle classification and

526 averaging procedures (actual samples will require a lower particle density than illustrated in
527 this figure to minimize overlapping of PSFs of fluorescent molecules of the same type).
528

Acknowledgements

We are grateful to E. Yvonne Jones (Division of Structural Biology, Wellcome Trust Centre for Human Genetics, University of Oxford, UK), and Ilan Davis and Ian Dobbie (Micron Advanced Bioimaging Unit, Department of Biochemistry, University of Oxford, UK) for their constant support; and to Marc Brecht (University of Tübingen, Germany), Alexander Rigort (FEI, Gräfelfing, Germany) and Michael Schwertner (Linkam Scientific Instruments, Surrey, UK) for stimulating discussions about future cryo-CLEM approaches.

Funding

This work was supported by a Wellcome Trust Senior Research Fellowship [107806/Z/15/Z to K.G.], a Human Frontiers grant (RGP0055/2015 to K.G.), the Wellcome Trust core award to the Wellcome Trust Centre for Human Genetics [090532/Z/09/Z] and the Micron Strategic Award from the Wellcome Trust [107457/Z/15/Z].

Abbreviations

CLEM, correlative light and electron microscopy
cryo-FM, fluorescence cryo-microscopy
cryo-EM, electron cryo-microscopy
CEMOVIS, electron cryo-microscopy of vitreous sections
FIB, focused ion beam
NA, numerical aperture
PSF, point spread function
STED, stimulated emission depletion
SIM, structured illumination microscopy
SMLM, single molecule localization microscopy
STORM, stochastic optical reconstruction microscopy
(F)PALM, (fluorescence) photoactivated localization microscopy
dSTORM, direct STORM
SPDM, spectral position determination microscopy
GSDIM, ground state depletion followed by individual molecule return
ESS, excited state saturation

References

Al-Amoudi, A., Chang, J.J., Leforestier, A., McDowall, A., Salamin, L.M., Norlen, L.P.O., Richter, K., Blanc, N.S., Studer, D. and Dubochet, J. (2004) Cryo-electron microscopy of vitreous sections. Embo J. **23**, 3583-3588

Ando, R., Mizuno, H. and Miyawaki, A. (2004) Regulated fast nucleocytoplasmic shuttling observed by reversible protein highlighting. Science **306**, 1370-1373

Aquino, D., Schönle, A., Geisler, C., von Middendorff, C., Wurm, C.A., Okamura, Y., Lang, T., Hell, S.W. and Egner, A. (2011) Two-color nanoscopy of three-dimensional volumes by 4Pi detection of stochastically switched fluorophores. Nat. Methods **8**, 353-359

Arnold, J., Mahamid, J., Lučić, V., de Marco, A., Fernandez, J.J., Laugks, T., Mayer, T., Hyman, A.A., Baumeister, W. and Plitzko, J.M. (2016) Site-specific cryo-focused ion beam sample preparation guided by 3D correlative microscopy. Biophys. J. **110**, 860-869

Betzig, E., Patterson, G.H., Sougrat, R., Lindwasser, O.W., Olenych, S., Bonifacino, J.S., Davidson, M.W., Lippincott-Schwartz, J. and Hess, H.F. (2006) Imaging intracellular fluorescent proteins at nanometer resolution. Science **313**, 1642-1645

Betzig, E. (2015) Single molecules, cells, and super-resolution optics (Nobel lecture). Angew. Chem.-Int. Edit. **54**, 8034-8053

Bharat, T.A.M., Russo, C.J., Löwe, J., Passmore, L.A. and Scheres, S.H.W. (2015) Advances in single-particle electron cryomicroscopy structure determination applied to sub-tomogram averaging. Structure **23**, 1743-1753

Bleck, C.K.E., Merz, A., Gutierrez, M.G., Walther, P., Dubochet, J., Zuber, B. and Griffiths, G. (2010) Comparison of different methods for thin section EM analysis of *Mycobacterium smegmatis*. J. Microsc. **237**, 23-38

Briegel, A., Chen, S.Y., Koster, A.J., Plitzko, J.M., Schwartz, C.L. and Jensen, G.J. (2010) Correlated light and electron cryo-microscopy. In Methods in Enzymology, Vol 481:

586 Cryo-EM, Part A - Sample Preparation and Data Collection (Jensen, G. ed.), pp. 317-
587 341, Elsevier, San Diego, CA
588 Brüggeller, P. and Mayer, E. (1980) Complete vitrification in pure liquid water and dilute
589 aqueous-solutions. Nature **288**, 569-571
590 Callaway, E. (2015) The revolution will not be crystallized. Nature **525**, 172-174
591 Carlson, D.B. and Evans, J.E. (2011) Low-cost cryo-light microscopy stage fabrication for
592 correlated light/electron microscopy. J. Vis. Exp. **52**, e2909
593 Carzaniga, R., Domart, M.C., Duke, E. and Collinson, L.M. (2014) Correlative cryo-
594 fluorescence and cryo-soft X-ray tomography of adherent cells at European synchrotrons.
595 In Correlative Light and Electron Microscopy II (Müller-Reichert, T. and Verkade, P.
596 eds.), pp. 151-178, Academic Press, Burlington, MA
597 Castro-Hartmann, P., Heck, G., Eltit, J.M., Fawcett, P. and Samso, M. (2013) The ArrayGrid:
598 A methodology for applying multiple samples to a single TEM specimen grid.
599 Ultramicroscopy **135**, 105-112
600 Chang, Y.W., Chen, S.Y., Tocheva, E.I., Treuner-Lange, A., Löbach, S., Søgaard-Andersen,
601 L. and Jensen, G.J. (2014) Correlated cryogenic photoactivated localization microscopy
602 and cryo-electron tomography. Nat. Methods **11**, 737-739
603 Comolli, L.R., Duarte, R., Baum, D., Luef, B., Downing, K.H., Larson, D.M., Csencsits, R.
604 and Banfield, J.F. (2012) A portable cryo-plunger for on-site intact cryogenic microscopy
605 sample preparation in natural environments. Microsc. Res. Tech. **75**, 829-836
606 Creemers, T.M.H., Lock, A.J., Subramaniam, V., Jovin, T.M. and Völker, S. (2000)
607 Photophysics and optical switching in green fluorescent protein mutants. Proc. Natl.
608 Acad. Sci. U. S. A. **97**, 2974-2978
609 de Boer, P., Hoogenboom, J.P. and Giepmans, B.N.G. (2015) Correlated light and electron
610 microscopy: ultrastructure lights up! Nat. Methods **12**, 503-513

611 Do, M., Isaacson, S.A., McDermott, G., Le Gros, M.A. and Larabell, C.A. (2015) Imaging and
612 characterizing cells using tomography. Arch. Biochem. Biophys. **581**, 111-121
613 Dobro, M.J., Melanson, L.A., Jensen, G.J. and McDowall, A.W. (2010) Plunge freezing for
614 electron cryomicroscopy. In Methods in Enzymology, Vol 481: Cryo-EM, Part A -
615 Sample Preparation and Data Collection, pp. 63-82, Elsevier, San Diego, CA
616 Dubochet, J. and McDowall, A.W. (1981) Vitrification of pure water for electron microscopy.
617 J. Microsc. **124**, 3-4
618 Dubochet, J., Adrian, M., Chang, J.J., Homo, J.C., Lepault, J., McDowall, A.W. and Schultz,
619 P. (1988) Cryo-electron microscopy of vitrified specimens. Q. Rev. Biophys. **21**, 129-
620 228
621 Dubochet, J. (2007) The physics of rapid cooling and its implications for cryoimmobilization
622 of cells. In Cellular Electron Microscopy (McIntosh, J.R. ed.), pp. 7-21, Elsevier
623 Academic Press, San Diego
624 Dubochet, J. (2012) Cryo-EM - the first thirty years. J. Microsc. **245**, 221-224
625 Dubochet, J. (2016) A reminiscence about early times of vitreous water in electron
626 cryomicroscopy. Biophys. J. **110**, 756-757
627 Egelman, E.H. (2016) The current revolution in cryo-EM. Biophys. J. **110**, 1008-1012
628 Eggeling, C., Willig, K.I. and Barrantes, F.J. (2013) STED microscopy of living cells - new
629 frontiers in membrane and neurobiology. J. Neurochem. **126**, 203-212
630 Eisenstein, M. (2016) The field that came in from the cold. Nat. Methods **13**, 19-22
631 Engelmann, R., Anhut, T., Kleppe, I. and Weisshart, K. (2014) Airyscanning: evoking the full
632 potential of confocal microscopy. G.I.T. Imaging & Microscopy **3**, 20-21
633 Faro, A.R., Adam, V., Carpentier, P., Darnault, C., Bourgeois, D. and de Rosny, E. (2010)
634 Low-temperature switching by photoinduced protonation in photochromic fluorescent
635 proteins. Photochem. Photobiol. Sci. **9**, 254-262

Fölling, J., Bossi, M., Bock, H., Medda, R., Wurm, C.A., Hein, B., Jakobs, S., Eggeling, C. and Hell, S.W. (2008) Fluorescence nanoscopy by ground-state depletion and single-molecule return. Nat. Methods **5**, 943-945

Fonta, C.L. and Humbel, B.M. (2015) Correlative microscopy. Arch. Biochem. Biophys. **581**, 98-110

Fornasiero, E.F. and Opazo, F. (2015) Super-resolution imaging for cell biologists. Bioessays **37**, 436-451

Frederik, P.M. and Hubert, D.H.W. (2005) Cryoelectron microscopy of liposomes. In Methods in Enzymology, Vol. 391: Liposomes, Part E (Duzgunes, N. ed.), pp. 431-448, Elsevier, San Diego, CA

Giske, A. (2007) CryoSTED Microscopy-A New Spectroscopic Approach for Improving the Resolution of STED Microscopy Using Low Temperature. PhD, Ruperto-Carola University of Heidelberg, Heidelberg

Glaeser, R.M. (2016) How good can cryo-EM become? Nat. Methods **13**, 28-32

Glaeser, R.M., Han, B.G., Csencsits, R., Killilea, A., Pulk, A. and Cate, J.H.D. (2016) Factors that influence the formation and stability of thin, cryo-EM specimens. Biophys. J. **110**, 749-755

Gould, T.J., Gunewardene, M.S., Gudheti, M.V., Verkhusha, V.V., Yin, S.R., Gosse, J.A. and Hess, S.T. (2008) Nanoscale imaging of molecular positions and anisotropies. Nat. Methods **5**, 1027-1030

Gustafsson, M.G.L., Agard, D.A. and Sedat, J.W. (1995) Sevenfold improvement of axial resolution in 3D widefield microscopy using 2 objective lenses. In Three-Dimensional Microscopy: Image Acquisition and Processing II (Wilson, T. and Cogswell, C.J. eds.), pp. 147-156, Proceedings of the Society of Photo-Optical Instrumentation Engineers (SPIE), San Jose, CA

661 Gustafsson, M.G.L. (2000) Surpassing the lateral resolution limit by a factor of two using
662 structured illumination microscopy. J. Microsc. **198**, 82-87
663 Gustafsson, M.G.L. (2005) Nonlinear structured-illumination microscopy: Wide-field
664 fluorescence imaging with theoretically unlimited resolution. Proc. Natl. Acad. Sci. U.
665 S. A. **102**, 13081-13086
666 Han, H.M., Zuber, B. and Dubochet, J. (2008) Compression and crevasses in vitreous sections
667 under different cutting conditions. J. Microsc. **230**, 167-171.
668 Heilemann, M., van de Linde, S., Schüttpelz, M., Kasper, R., Seefeldt, B., Mukherjee, A.,
669 Tinnefeld, P. and Sauer, M. (2008) Subdiffraction-resolution fluorescence imaging with
670 conventional fluorescent probes. Angew. Chem.-Int. Edit. **47**, 6172-6176
671 Hein, B., Willig, K.I., Wurm, C.A., Westphal, V., Jakobs, S. and Hell, S.W. (2010) Stimulated
672 emission depletion nanoscopy of living cells using SNAP-tag fusion proteins. Biophys.
673 J. **98**, 158-163
674 Heintzmann, R. and Cremer, C. (1999) Laterally modulated excitation microscopy:
675 Improvement of resolution by using a diffraction grating. P. Soc. Photo-Opt. Ins. **3568**,
676 185-196
677 Hell, S. and Stelzer, E.H.K. (1992) Fundamental improvement of resolution with a 4Pi-
678 confocal fluorescence microscope using 2-photon excitation. Opt. Commun. **93**, 277-282
679 Hell, S.W., Stelzer, E.H.K., Lindek, S. and Cremer, C. (1994) Confocal microscopy with an
680 increased detection aperture - type-b 4Pi confocal microscopy. Opt. Lett. **19**, 222-224
681 Hell, S.W. and Wichmann, J. (1994) Breaking the diffraction resolution limit by stimulated
682 emission: stimulated-emission-depletion fluorescence microscopy. Opt. Lett. **19**, 780-
683 782
684 Hell, S.W. (2009) Microscopy and its focal switch. Nat. Methods **6**, 24-32

685 Hell, S.W., Sahl, S.J., Bates, M., Zhuang, X.W., Heintzmann, R., Booth, M.J., Bewersdorf, J.,
686 Shtengel, G., Hess, H., Tinnefeld, P., Honigmann, A., Jakobs, S., Testa, I., Cognet, L.,
687 Lounis, B., Ewers, H., Davis, S.J., Eggeling, C., Klenerman, D., Willig, K.I., Vicidomini,
688 G., Castello, M., Diaspro, A. and Cordes, T. (2015) The 2015 super-resolution
689 microscopy roadmap. J. Phys. D-Appl. Phys. **48**, 443001
690 Hess, S.T., Girirajan, T.P.K. and Mason, M.D. (2006) Ultra-high resolution imaging by
691 fluorescence photoactivation localization microscopy. Biophys. J. **91**, 4258-4272
692 Huang, F., Hartwich, T.M.P., Rivera-Molina, F.E., Lin, Y., Duim, W.C., Long, J.J., Uchil,
693 P.D., Myers, J.R., Baird, M.A., Mothes, W., Davidson, M.W., Toomre, D. and
694 Bewersdorf, J. (2013) Video-rate nanoscopy using sCMOS camera-specific single-
695 molecule localization algorithms. Nat. Methods **10**, 653-658
696 Huebinger, J., Han, H.M., Hofnagel, O., Vetter, I.R., Bastiaens, P.I.H. and Grabenbauer, M.
697 (2016) Direct measurement of water states in cryopreserved cells reveals tolerance
698 toward ice crystallization. Biophys. J. **110**, 840-849
699 Hussels, M., Konrad, A. and Brecht, M. (2012) Confocal sample-scanning microscope for
700 single-molecule spectroscopy and microscopy with fast sample exchange at cryogenic
701 temperatures. Rev. Sci. Instrum. **83**, 123706
702 Inagawa, H., Toratani, Y., Motohashi, K., Nakamura, I., Matsushita, M. and Fujiyoshi, S.
703 (2015) Reflecting microscope system with a 0.99 numerical aperture designed for three-
704 dimensional fluorescence imaging of individual molecules at cryogenic temperatures.
705 Sci. Rep. **5**, 12833
706 Irobalieva, R.N., Martins, B. and Medalia, O. (2016) Cellular structural biology as revealed by
707 cryo-electron tomography. J. Cell Sci. **129**, 469-476

Jain, T., Sheehan, P., Crum, J., Carragher, B. and Potter, C.S. (2012) Spotiton: A prototype for an integrated inkjet dispense and vitrification system for cryo-TEM. J. Struct. Biol. **179**, 68-75

Johnson, E., Seiradake, E., Jones, E.Y., Davis, I., Grünewald, K. and Kaufmann, R. (2015) Correlative in-resin super-resolution and electron microscopy using standard fluorescent proteins. Sci. Rep. **5**, 9583

Jones, S.A., Shim, S.H., He, J. and Zhuang, X.W. (2011) Fast, three-dimensional super-resolution imaging of live cells. Nat. Methods **8**, 499-508

Jun, S.M., Ke, D.X., Debiec, K., Zhao, G.P., Meng, X., Ambrose, Z., Gibson, G.A., Watkins, S.C. and Zhang, P.J. (2011) Direct visualization of HIV-1 with correlative live-cell microscopy and cryo-electron tomography. Structure **19**, 1573-1581

Kaufmann, R., Hagen, C. and Grünewald, K. (2014a) Fluorescence cryo-microscopy: current challenges and prospects. Curr. Opin. Chem. Biol. **20**, 86-91

Kaufmann, R., Schellenberger, P., Seiradake, E., Dobbie, I.M., Jones, E.Y., Davis, I., Hagen, C. and Grünewald, K. (2014b) Super-resolution microscopy using standard fluorescent proteins in intact cells under cryo-conditions. Nano Lett. **14**, 4171-4175

Korogod, N., Petersen, C.C.H. and Knott, G.W. (2015) Ultrastructural analysis of adult mouse neocortex comparing aldehyde perfusion with cryo fixation. eLife **4**, e05793

Kühlbrandt, W. (2014) The resolution revolution. Science **343**, 1443-1444

Kühlbrandt, W. (2015) Structure and function of mitochondrial membrane protein complexes. BMC Biol. **13**, 89

Le Gros, M.A., McDermott, G., Uchida, M., Knoechel, C.G. and Larabell, C.A. (2009) High-aperture cryogenic light microscopy. J. Microsc. **235**, 1-8

731 Lemmer, P., Gunkel, M., Baddeley, D., Kaufmann, R., Urich, A., Weiland, Y., Reymann, J.,
732 Müller, P., Hausmann, M. and Cremer, C. (2008) SPDM: light microscopy with single-
733 molecule resolution at the nanoscale. Appl. Phys. B-Lasers Opt. **93**, 1-12
734 Lew, M.D. and Moerner, W.E. (2014) Azimuthal polarization filtering for accurate, precise,
735 and robust single-molecule localization microscopy. Nano Lett. **14**, 6407-6413
736 Li, D., Shao, L., Chen, B.C., Zhang, X., Zhang, M.S., Moses, B., Milkie, D.E., Beach, J.R.,
737 Hammer, J.A., Pasham, M., Kirchhausen, T., Baird, M.A., Davidson, M.W., Xu, P.Y.
738 and Betzig, E. (2015a) Extended-resolution structured illumination imaging of endocytic
739 and cytoskeletal dynamics. Science **349**, 944-944
740 Li, W.X., Stein, S.C., Gregor, I. and Enderlein, J. (2015b) Ultra-stable and versatile widefield
741 cryo-fluorescence microscope for single-molecule localization with sub-nanometer
742 accuracy. Opt. Express **23**, 3770-3783
743 Liu, B., Xue, Y.H., Zhao, W., Chen, Y., Fan, C.Y., Gu, L.S., Zhang, Y.D., Zhang, X., Sun, L.,
744 Huang, X.J., Ding, W., Sun, F., Ji, W. and Xu, T. (2015) Three-dimensional super-
745 resolution protein localization correlated with vitrified cellular context. Sci. Rep. **5**,
746 13017
747 Lu, Z.H., Shaikh, T.R., Barnard, D., Meng, X., Mohamed, H., Yassin, A., Mannella, C.A.,
748 Agrawal, R.K., Lu, T.M. and Wagenknecht, T. (2009) Monolithic microfluidic mixing-
749 spraying devices for time-resolved cryo-electron microscopy. J. Struct. Biol. **168**, 388-
750 395
751 Lučić, V., Förster, F. and Baumeister, W. (2005) Structural studies by electron tomography:
752 from cells to molecules. Annu. Rev. Biochem. **74**, 833-865
753 Marko, M., Hsieh, C., Moberlychan, W., Mannella, C.A. and Frank, J. (2006) Focused ion
754 beam milling of vitreous water: prospects for an alternative to cryo-ultramicrotomy of
755 frozen-hydrated biological samples. J. Microsc. **222**, 42-47

McDonald, K.L. (2014) Out with the old and in with the new: rapid specimen preparation procedures for electron microscopy of sectioned biological material. Protoplasma **251**, 429-448

Mejia, Y.X., Feindt, H., Zhang, D., Steltenkamp, S. and Burg, T.P. (2014) Microfluidic cryofixation for correlative microscopy. Lab Chip **14**, 3281-3284

Mielanczyk, L., Matysiak, N., Michalski, M., Buldak, R. and Wojnicz, R. (2014) Closer to the native state. Critical evaluation of cryo-techniques for Transmission Electron Microscopy: preparation of biological samples. Folia Histochem. Cytobiol. **52**, 1-17

Moerner, W.E. and Orrit, M. (1999) Illuminating single molecules in condensed matter. Science **283**, 1670-1676

Moerner, W.E. (2002) A dozen years of single-molecule spectroscopy in physics, chemistry, and biophysics. J. Phys. Chem. B **106**, 910-927

Moor, H. (1987) Theory and practice of high pressure freezing. In Cryotechniques in Biological Electron Microscopy (Steinbrecht, R.A. and Zierold, K. eds.), pp. 175-191, Springer, Berlin

Morgenstern, E. (1991) Aldehyde fixation causes membrane vesiculation during platelet exocytosis - a freeze-substitution study. Scanning Microsc. **5**, S109-S115

Nogales, E. (2016) The development of cryo-EM into a mainstream structural biology technique. Nat. Methods **13**, 24-27

Patterson, G.H. and Lippincott-Schwartz, J. (2002) A photoactivatable GFP for selective photolabeling of proteins and cells. Science **297**, 1873-1877

Resch, G.P., Brandstetter, M., Pickl-Herk, A.M., Königsmaier, L., Wonesch, V.I. and Urban, E. (2011) Immersion freezing of biological specimens: Rationale, principles, and instrumentation. Cold Spring Harb. Protoc. **2011**, 778-782

780 Riehle, U. and Hoechli, M. (1973) The theory and technique of high pressure freezing. In
781 Freeze-Etching Techniques and Applications (Benedetti, E.L. and Favard, P. eds.), pp.
782 31-61, Société française de microscopie électronique, Paris
783 Rigort, A., Bäuerlein, F.J.B., Leis, A., Gruska, M., Hoffmann, C., Laugks, T., Böhm, U.,
784 Eibauer, M., Gnaegi, H., Baumeister, W. and Plitzko, J.M. (2010) Micromachining tools
785 and correlative approaches for cellular cryo-electron tomography. J. Struct. Biol. **172**,
786 169-179
787 Rigort, A., Kirmse, R., Döring, V., Kalkbrenner, T. and Wolleschensky, R. (2015a) Cryo-
788 confocal imaging with Airyscan improving resolution and signal-to-noise in cryo-
789 fluorescence microscopy. CZ Appl. Notes **5**, 1-8
790 Rigort, A., Kirmse, R., Döring, V., Schwertner, M. and Wolleschensky, R. (2015b) Imaging of
791 vitrified biological specimens by confocal cryo-fluorescence microscopy and cryo-
792 FIB/SEM tomography. Microsc. Microanal. **21**, 1121-1122
793 Rigort, A. and Plitzko, J.M. (2015) Cryo-focused-ion-beam applications in structural biology.
794 Arch. Biochem. Biophys. **581**, 122-130
795 Rodriguez, J.A., Ivanova, M.I., Sawaya, M.R., Cascio, D., Reyes, F.E., Shi, D., Sangwan, S.,
796 Guenther, E.L., Johnson, L.M., Zhang, M., Jiang, L., Arbing, M.A., Nannenga, B.L.,
797 Hattne, J., Whitelegge, J., Brewster, A.S., Messerschmidt, M., Boutet, B., Sauter, N.K.,
798 Gonen, T. and Eisenberg, D.S. (2015) Structure of the toxic core of alpha-synuclein from
799 invisible crystals. Nature **525**, 486-490
800 Rubino, S., Melin, P., Spellward, P. and Leifer, K. (2014) Cryo-electron microscopy specimen
801 preparation by means of a focused ion beam. J. Vis. Exp. **89**, e51463
802 Rust, M.J., Bates, M. and Zhuang, X.W. (2006) Sub-diffraction-limit imaging by stochastic
803 optical reconstruction microscopy (STORM). Nat. Methods **3**, 793-795

804 Sartori, A., Gatz, R., Beck, F., Rigort, A., Baumeister, W. and Plitzko, J.M. (2007) Correlative
805 microscopy: bridging the gap between fluorescence light microscopy and cryo-electron
806 tomography. J. Struct. Biol. **160**, 135-145
807 Schellenberger, P., Kaufmann, R., Siebert, C.A., Hagen, C., Wodrich, H. and Grünewald, K.
808 (2014) High-precision correlative fluorescence and electron cryo microscopy using two
809 independent alignment markers. Ultramicroscopy **143**, 41-51
810 Schneider, G., Guttmann, P., Rehbein, S., Werner, S. and Follath, R. (2012) Cryo X-ray
811 microscope with flat sample geometry for correlative fluorescence and nanoscale
812 tomographic imaging. J. Struct. Biol. **177**, 212-223
813 Schorb, M. and Briggs, J.A.G. (2014) Correlated cryo-fluorescence and cryo-electron
814 microscopy with high spatial precision and improved sensitivity. Ultramicroscopy **143**,
815 24-32
816 Schur, F.K.M., Hagen, W.J.H., Rumlova, M., Ruml, T., Müller, B., Kräusslich, H.G. and
817 Briggs, J.A.G. (2015) Structure of the immature HIV-1 capsid in intact virus particles at
818 8.8 angstrom resolution. Nature **517**, 505-508
819 Schwartz, C.L., Sarbash, V.I., Ataullakhanov, F.I., McIntosh, J.R. and Nicastro, D. (2007)
820 Cryo-fluorescence microscopy facilitates correlations between light and cryo-electron
821 microscopy and reduces the rate of photobleaching. J. Microsc. **227**, 98-109
822 Shao, L., Kner, P., Rego, E.H. and Gustafsson, M.G.L. (2011) Super-resolution 3D microscopy
823 of live whole cells using structured illumination. Nat. Methods **8**, 1044-1046
824 Smith, E.A., McDermott, G., Do, M., Leung, K., Panning, B., Le Gros, M.A. and Larabell,
825 C.A. (2014) Quantitatively imaging chromosomes by correlated cryo-fluorescence and
826 soft X-ray tomographies. Biophys. J. **107**, 1988-1996
827 Strnad, M., Elsterová, J., Schrenková, J., Vancová, M., Rego, R.O.M., Grubhoffer, L. and
828 Nebesářová, J. (2015) Correlative cryo-fluorescence and cryo-scanning electron

829 microscopy as a straightforward tool to study host-pathogen interactions. Sci. Rep. **5**,
830 18029
831 Subramaniam, S., Kühlbrandt, W. and Henderson, R. (2016) CryoEM at IUCrJ: a new era.
832 IUCrJ **3**, 3-7
833 Sydor, A.M., Czymmek, K.J., Puchner, E.M. and Mennella, V. (2015) Super-resolution
834 microscopy: From single molecules to supramolecular assemblies. Trends Cell Biol. **25**,
835 730-748
836 Tan, Y.Z., Cheng, A., Potter, C.S. and Carragher, B. (2016) Automated data collection in single
837 particle electron microscopy. Microscopy **65**, 43-56
838 Taylor, K.A. and Glaeser, R.M. (1974) Electron diffraction of frozen, hydrated protein crystals.
839 Science **186**, 1036-1037
840 Timmermans, F.J. and Otto, C. (2015) Review of integrated correlative light and electron
841 microscopy. Rev. Sci. Instrum. **86**, 011501
842 Tivol, W.F., Briegel, A. and Jensen, G.J. (2008) An improved cryogen for plunge freezing.
843 Microsc. Microanal. **14**, 375-379
844 Tychinskii, V.P., Kufal, G.E., Vyshenskaya, T.V., Perevedentseva, E.V. and Nikandrov, S.L.
845 (1997) Measurements of submicron structures with the Airyscan laser phase microscope.
846 Quantum Electron. **27**, 735-739
847 van Driel, L.F., Valentijn, J.A., Valentijn, K.M., Koning, R.I. and Koster, A.J. (2009) Tools
848 for correlative cryo-fluorescence microscopy and cryo-electron tomography applied to
849 whole mitochondria in human endothelial cells. Eur. J. Cell Biol. **88**, 669-684
850 Watanabe, S., Punge, A., Hollopeter, G., Willig, K.I., Hobson, R.J., Davis, M.W., Hell, S.W.
851 and Jorgensen, E.M. (2011) Protein localization in electron micrographs using
852 fluorescence nanoscopy. Nat. Methods **8**, 80-84

Weinhausen, B., Saldanha, O., Wilke, R.N., Dammann, C., Priebe, M., Burghammer, M., Sprung, M. and Köster, S. (2014) Scanning X-ray nanodiffraction on living eukaryotic cells in microfluidic environments. Phys. Rev. Lett. **112**, 088102

Weisenburger, S., Jing, B., Renn, A. and Sandoghdar, V. (2013) Cryogenic localization of single molecules with Angstrom precision. In Nanoimaging and Nanospectroscopy (Verma, P.E., A ed.), pp. 88150D, SPIE-Int. Soc. Opt. Engineer., Bellingham, WA

Weisenburger, S., Jing, B., Hänni, D., Reymond, L., Schuler, B., Renn, A. and Sandoghdar, V. (2014) Cryogenic colocalization microscopy for nanometer-distance measurements. ChemPhysChem **15**, 763-770

Weisenburger, S. and Sandoghdar, V. (2015) Light microscopy: an ongoing contemporary revolution. Contemp. Phys. **56**, 123-143

Westphal, V., Rizzoli, S.O., Lauterbach, M.A., Kamin, D., Jahn, R. and Hell, S.W. (2008) Video-rate far-field optical nanoscopy dissects synaptic vesicle movement. Science **320**, 246-249

Wildanger, D., Medda, R., Kastrup, L. and Hell, S.W. (2009) A compact STED microscope providing 3D nanoscale resolution. J. Microsc. **236**, 35-43

Xu, D.L., Jiang, T., Li, A.A., Hu, B.H., Feng, Z., Gong, H., Zeng, S.Q. and Luo, Q.M. (2013) Fast optical sectioning obtained by structured illumination microscopy using a digital mirror device. J. Biomed. Opt. **18**, 060503

Xu, K., Babcock, H.P. and Zhuang, X.W. (2012) Dual-objective STORM reveals three-dimensional filament organization in the actin cytoskeleton. Nat. Methods **9**, 185-188

Yang, B., Trebbia, J.B., Baby, R., Tamarat, P. and Lounis, B. (2015) Optical nanoscopy with excited state saturation at liquid helium temperatures. Nat. Photonics **9**, 658-662

876 Zondervan, R., Kulzer, F., Orlinskii, S.B. and Orrit, M. (2003) Photoblinking of rhodamine 6G
877 in poly(vinyl alcohol): Radical dark state formed through the triplet. J. Phys. Chem. A
878 **107**, 6770-6776

879